Unified models for adaptive OFDM systems when QAM or PSK modulation is applied

ARTICLE *in* EUROPEAN TRANSACTIONS ON TELECOMMUNICATIONS · NOVEMBER 2007

Impact Factor: 1.35 · DOI: 10.1002/ett.1173 · Source: DBLP

2 AUTHORS:

Costas Assimakopoulos
Aristotle University of Thessaloniki
18 PUBLICATIONS **43** CITATIONS
SEE PROFILE

Fotini-Niovi Pavlidou
Aristotle University of Thessaloniki
168 PUBLICATIONS **1,294** CITATIONS
SEE PROFILE

EUROPEAN TRANSACTIONS ON TELECOMMUNICATIONS
Euro. Trans. Telecomms. 2007; **18**:777–790
Published online 9 February 2007 in Wiley InterScience
(www.interscience.wiley.com). DOI: 10.1002/ett.1173

Transmission Systems

Unified models for adaptive OFDM systems when QAM or PSK modulation is applied

Costas Assimakopoulos* and F.-N. Pavlidou

Department of Electrical & Computer Engineering, Aristotle University of Thessaloniki, Panepistimioupolis of Thessaloniki, 54124, Thessaloniki, Greece

SUMMARY

In this paper, the solutions of the major bit-loading problems that are found in the literature, are unified into simple equations (models). These equations give an insight of the affection of the channel over a multicarrier system. Moreover, the models allow the transition from the solution of one loading problem to the solution of the others. The models are dependent on the modulation type that is used. We examine the quadrature amplitude modulation (QAM) modulated orthogonal frequency division multiplexing (OFDM), and the phase shift keying (PSK)-modulated OFDM systems. For each modulation type, the continuous throughput model is extracted. The continuous throughput model refers to a system that its subcarriers can be loaded with non-integer number of bits. The non-integer bit distribution can then be rounded to integers, using a rounding method. The models except from the calculation of the optimised quantities (total data rate, total power and symbol error rate) without the need of running a loading algorithm to its extent, provide a means to manipulate a whole multicarrier system in a way similar to single-carrier system.

1. INTRODUCTION

The wireless spectrum is a limited resource. As modern wireless communications need to occupy more and more spectrum, spectrally efficient modulation is imperative. A widespread solution is orthogonal frequency division multiplexing (OFDM). An OFDM system consists of a set of parallel subcarriers, which are mutually orthogonal. It has been proved that significant performance improvement can be achieved, if the number of bits that each subcarrier is loaded with and the transmission power is adapted, according to the subchannel to noise ratios (STNR's) [1, 2]. Of course, this means that the transmitter is aware of the instantaneous channel gains and noise characteristics of all of the subcarriers. This demands feedback from the receiver. Moreover, the receiver should be aware of the different modulation modes per subcarrier, in order to demodulate the information correctly.

The parameters to be considered for a multicarrier loaded system are the total data rate R_T, the total transmission power P_T per OFDM symbol and the overall probability of symbol error P_{err}. These parameters are named global parameters [3]. One global parameter is being optimised (either maximised or minimised), whereas the other two impose the constraints of the problem. The algorithms proposed in the literature so far aim to maximise the total data rate, minimise the error rate or the total transmission power. According to the special application where the adaptive OFDM is used, several other constraints are added. For instance, non-integer bit distributions are

* Correspondence to: Costas Assimakopoulos, Department of Electrical & Computer Engineering, Aristotle University of Thessaloniki, Panepistimioupolis of Thessaloniki, 54124, Thessaloniki, Greece. E-mail: casim@eng.auth.gr

Received 18 May 2005
Revised 3 May 2006
Accepted 14 June 2006

practically unacceptable [4]. This is due to the fact that quadrature amplitude modulation (QAM) or phase shift keying (PSK) leads to integer bit assignment per symbol. Moreover, legislation imposes bounds to the maximum transmission power $P_{\max}$ at certain frequencies. The maximum acceptable power leads to restrictions to the maximum bit load per subcarrier [5]. This is also a constraint to the optimisation problem.

There are several algorithms in the literature. Basically, two main categories of those algorithms exist. The first category includes algorithms that solve the optimisation problems analytically [4, 6, 7], relaxing the constraint for integer bit distributions. The resulting system is named continuous throughput because the analytical equations for the bit distributions lead to non-integers. Then using a rounding method [6, 8], they convert the non-integer bit distribution to integer. The other category includes algorithms that assign integer number of bits to the subcarriers [9–12], based on the greedy approach.

Piazzo in Reference [3] has proved that a system, which is optimised with respect to one of the global parameters, is also optimum with respect to the other two (equivalent solutions). Those solutions belong to a set that is named globally optimal set. The analysis is focused mainly in the continuous throughput system. In this case, Piazzo claims a theorem that unifies the solutions of the optimisation problems. The practical outcome of the theorem is the existence of 'operators' that allow transferring from one optimised system to the other. Since all optimisation problems do not have the same complexity, solving the simplest of the three problems is equivalent to solving any of the other two.

In this paper, we move a step further, proving that the solutions are not just equivalent but they are identical. This formalisation is going to be used to extract a unified model that describes any bit-loaded multicarrier system. This unified model is the 'operator' that Piazzo claims in Reference [3] and allows transferring from the solution of one optimisation problem to the other. Of course, the operator depends on the modulation type.

However, before reaching the unified models, the system model is introduced in detail in Section 2. In Section 3, the optimisation problems are formed and the equivalence of the different problems is explained. In Sections 4 and 5, the bit and power distributions for QAM- and PSK-modulated OFDM systems are extracted for each optimisation problem. The additional feature is that it is proved that the solutions of the optimisation problems are identical. Then, running simulations on a common channel, it is verified experimentally that the three optimisation problems lead to identical non-integer bit distributions. Those simulations confirm practically what we expected from the preceding theoretic analysis and enforce the argument about the unified solution. Exploiting the analytical results for QAM and PSK multicarrier systems, we construct the unified models that describe the overall system performance and implicate the global parameters of the systems on simple equations. These equations, solved for one of the three global parameters, can give the needed optimised quantity as a function of the other two, without the need of running the loading algorithms to its extend. Moreover, the equations provide a deep insight of the channel's influence on the system and, in fact, summarise it.

The unified models ('operators') for the examined modulation types are valid for continuous throughput systems. In many papers, the final integer bit distribution is obtained rounding the real number bit distribution. Applying a rounding algorithm, like the one proposed in Reference [8], the error rate performance of the integer throughput systems is obtained by simulations. Then, on the same graphs, the actual and the modelled symbol error rate curves are plotted. For both QAM–OFDM and PSK–OFDM systems, the continuous throughput models are rather close to the actual system performance.

2. SYSTEM MODEL

Assume that an OFDM system consists of N parallel subcarriers. Each subcarrier is modulated to transmit R_i bits (i is the subcarrier index) and suffers by fading that is different from subchannel to subchannel[†]. Let us use the notation $H_i(f_i)$ to express the subchannel's amplitude and phase influence on the ith subcarrier. The symbol P_i denotes the power transmission per subcarrier. So, the received signal has power per subcarrier given by Equation (1)

$$E_{r,i} = P_i |H_i(f_i)|^2 \tag{1}$$

We consider that every subcarrier is affected by additive white Gaussian noise of zero mean and variance n_i. For unit transmission power, the subchannel to noise ratio is given by Equation (2).

[†]Here, the word subchannel is not used alternatively for the word subcarrier, although in some papers, the two words are used mutually. The term subchannel, refers to the part of the physical channel dedicated to the specific subcarrier of the multicarrier system.

DOI:10.1002/ett

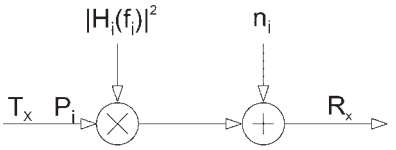

Figure 1. Subchannel model.

This parameter is going to be used often in the remainder of the paper as it summarises the channel gain and the noise effect per subchannel. The described subchannel model is shown in Figure 1.

$$g_i = \frac{|H_i(f_i)|^2}{n_i} \tag{2}$$

The subchannel to noise ratios are independent from each other as the channel's coherence bandwidth is assumed to be smaller than the subcarrier spacing. Moreover, perfect channel estimation is assumed and channel variations are slow and followed accurately by the channel equaliser.

The notation $P_{\text{error},i}$ is used for the symbol error rate (SER) at the ith subcarrier. We should evoke that on a subcarrier basis, the transmission power P_i, the bits per symbol R_i, the symbol error rate $P_{\text{error},i}$ and the subchannel to noise ratio g_i are connected through a function, either strictly describing or approximating the relationship between them. This equation depends on the modulation type that is used and in most cases, it entails the well-known $Q(x)$ function which is a strictly decreasing function.

Let $P_{\text{error},i} = f(R_i, \text{SNR}_i)$ be that function. Using Equations (1) and (2), the signal to noise ratio per subcarrier at the receiver is $\text{SNR}_i = g_i P_i$ and the error rate function can be turned into $P_{\text{error},i} = f(R_i, P_i, g_i)$ (for simplicity reasons, $f(R_i, P_i, g_i)$ will be written as $f_i(R_i, P_i)$ where the index i in the function f_i encloses the channel to noise ratio g_i that differs from subchannel to subchannel).

When QAM or PSK is used, the function f_i is continuous and strictly monotonous. Obviously, when $R_i = 0$, then, $P_i = 0$ which means that no power is transmitted from a subcarrier that is not loaded with bits.

The optimum system, concerning the error rate, demands the $P_{\text{error},i}$ to be equal among the different subcarriers. Otherwise, the highest error rate among the subcarriers would dominate Reference [6]. In most of the papers existing in the literature, equal SER among the subcarriers is demanded [5, 6, 10, 13, 14].

Therefore, the global parameters, that is the total data rate per OFDM symbol, the total transmitting power and the symbol error rate, are calculated, based on the subcarrier parameters using the following equations respectively:

$$R_{\text{T}} = \sum_{i=1}^{N} R_i \tag{3}$$

$$P_{\text{T}} = \sum_{i=1}^{N} P_i \tag{4}$$

$$P_{\text{err}} = P_{\text{error},i}, \quad \forall i \in [1, N] \tag{5}$$

3. OPTIMISATION PROBLEMS

The objective target is to optimise one of the global parameters, given the other two. Thus, three optimisation problems are formulated. The data rate maximisation problem for given total power budget $P_{\text{T}}^{(1)}$ and symbol error rate $P_{\text{err}}^{(1)}$, the power minimisation problem for fixed data rate $R_{\text{T}}^{(2)}$ and symbol error rate $P_{\text{err}}^{(2)}$, and the error minimisation problem for constraint total power budget $P_{\text{T}}^{(3)}$ and total bit rate $R_{\text{T}}^{(3)\ddagger}$. Before solving the optimisation problems, there are some notions from the set theory that should be claimed. Let us consider the set S of all possible adaptive OFDM systems for a given channel and modulation type.

A system is rate optimum if there is no other system, operating at the same global transmission power and the same SER, achieving higher global data rate. The data rate optimum systems form the set $\Omega_R \subset S$.

A system is power optimum if there is no other system, operating at the same global data rate and the same SER, requiring lower global transmission power. The power optimum systems form the set $\Omega_P \subset S$.

Finally, a system is error rate optimum if there is no other system, operating at the same global transmission power and the same total data rate, achieving lower error rate. The error rate optimum systems form the set $\Omega_\eta \subset S$.

The intersection of the three defined sets gives the set Ω_g of the so-called globally optimum systems $\Omega_g = \Omega_R \cap \Omega_P \cap \Omega_\eta$, that is systems optimum simultaneously with respect to all three global parameters. In Reference [3] the following theorem is proved:

‡The indexes (1), (2), (3) are used to distinguish the global parameters among the optimisation problems. For the rest of the paper, (1), (2), (3) are used for the data rate, power and SER optimisation problems, respectively.

DOI:10.1002/ett

Theorem 1: *Given a continuous throughput OFDM system the following results:* $\Omega_g \equiv \Omega_R \equiv \Omega_P \equiv \Omega_\eta$.

This theorem asserts that in the case of continuous throughput OFDM systems, an optimum system with respect to one of the global parameters is optimal with respect to the other two. For details about the preceding analysis and for the proof of the theorem, the reader can refer to Reference [3]. We repeat here the main points of this analysis for quick reference. The above theorem claims that the adaptive OFDM systems that are solutions of the three different optimisation problems are equivalent. For example solving the data rate problem for a specific channel and modulation type, it results in the bit distribution named $B = \{R_1^{(1)}, R_2^{(1)}, \ldots, R_N^{(1)}\}$ having global parameters $P_{\mathrm{T}}^{(1)}$, $P_{\mathrm{err}}^{(1)}$, $R_{\mathrm{T}}^{(1)}$. Solving the power minimisation problem results in the bit distribution $C = \{R_1^{(2)}, R_2^{(2)}, \ldots, R_N^{(2)}\}$ having global parameters, according to Theorem 1, $P_{\mathrm{T}}^{(2)} = P_{\mathrm{T}}^{(1)}$, $P_{\mathrm{err}}^{(2)} = P_{\mathrm{err}}^{(1)}$, $R_{\mathrm{T}}^{(2)} = R_{\mathrm{T}}^{(1)}$. This is what equivalence of the solutions of the optimisation problems means. Nevertheless, in this paper, we move a step further proving for QAM and PSK adaptive OFDM systems that the solutions are not equivalent but identical, that is $B \equiv C$.

4. QAM APPLICATION

In this section, we work on a system based on QAM. The optimisation problems are solved and the bit and power distributions are extracted. Finally, the unified bit-loading model for a QAM multicarrier system is formed. In a QAM system, the variables P_i, R_i and $P_{\mathrm{error},i}$ cannot be implicated in one equation. When R_i is an even number there is an analytic equation but when it is odd there is not. On the other hand, it has been proved [2, 15] that the symbol error probability for QAM is bounded by Equation (6).

$$P_{\mathrm{error},i} \leqslant 4Q\left(\sqrt{\frac{3P_i g_i}{2^{R_i}-1}}\right), \quad R_i \geqslant 1 \tag{6}$$

In our analysis (as in other papers too), the equality of the previous bound is used, expecting the theoretic optimum solution to be pessimistic, compared to the performance of a real adaptive multicarrier system. In order to manipulate Equation (6) easier, its argument that implicates the symbol error rate, the transmission power and the bits per subcarrier is isolated into Equation (7).

$$A = \frac{3P_i g_i}{2^{R_i}-1} \tag{7}$$

We demand the symbol error rate per subcarrier to be constant $P_{\mathrm{error},i} = P_{\mathrm{err}}$ and thus, $A = [Q^{-1}(P_{\mathrm{err}}/4)]^2$ is constant too.

Solving Equation (7) for R_i, the rate-power function for QAM is obtained in Equation (8)

$$R_i = \log_2\left(1 + \frac{3P_i g_i}{A}\right) \tag{8}$$

Equation (8) is strictly increasing and thus it is invertible. The inverse function is

$$P_i = \frac{2^{R_i}-1}{3g_i} A \tag{9}$$

4.1. Problem 1: Maximising data rate

Let us consider a system that has to maximise the total data rate, under the constraints that the total transmission power should not surpass a power budget and the SER is less than a fixed error rate. Since the target is to maximise the data rate, it would be necessary to exploit all the available power. Simultaneously, the error rate should be equal to the maximum tolerable. Thus, the constraints are not inequalities. The problem is formulated as follows:

$$\sum_{i=1}^{N} R_i \to \max \tag{10}$$

$$\sum_{i=1}^{N} P_i = P_{\mathrm{T}}^{(1)} \tag{11}$$

$$A^{(1)} = \frac{3P_i g_i}{2^{R_i}-1} \tag{12}$$

The problem is solved using the well-known Lagrange method. Formulating the objective function Φ_1

$$\Phi_1 = \sum_{i=1}^{N} R_i + \lambda_1 \sum_{i=1}^{N} P_i \tag{13}$$

and imposing its derivative towards P_i to be equal to zero, we get Equation (14). From Equations (14) and (8), its equivalent Equation (15) is obtained.

$$\frac{\partial R_i}{\partial P_i} = -\lambda_1 \tag{14}$$

$$\frac{1}{\ln 2 \cdot \left(\frac{A^{(1)}}{3g_i} + P_i\right)} = -\lambda_1 \tag{15}$$

DOI:10.1002/ett

Solving Equation (15) for P_i, the optimum power distribution for the ith subcarrier is

$$P_i = \frac{1}{\ln 2 \cdot (-\lambda_1)} - \frac{A^{(1)}}{3g_i} \tag{16}$$

Using the properties of the Leibnitz notation, Equation (14) results in

$$\frac{\partial P_i}{\partial R_i} = -\frac{1}{\lambda_1} \tag{17}$$

Substituting Equation (9) into Equation (17) and solving for R_i, the bit distribution of the system that optimises the total data rate is

$$R_i = \log_2\left(-\frac{3g_i}{A^{(1)} \ln 2 \cdot \lambda_1}\right) \tag{18}$$

Using Equation (16) and the power constraint (11), the Lagrange multiplier is calculated at Equation (19). Then substituting λ_1 in Equations (16) and (18), the general solution for the first optimisation problem is extracted.

$$-\lambda_1 = \frac{N}{\ln 2 \cdot \left(P_{\mathrm{T}}^{(1)} + \frac{A^{(1)}}{3}\sum_{i=1}^{N}\frac{1}{g_i}\right)} \tag{19}$$

Obviously, the power and bit distributions will be functions of the known quantities $P_{\mathrm{T}}^{(1)}$ and $A^{(1)}$.

$$P_i = \frac{P_{\mathrm{T}}^{(1)}}{N} + \frac{A^{(1)}}{3N}\sum_{l=1}^{N}\left(\frac{1}{g_l} - \frac{1}{g_i}\right), \quad P_i > 0 \tag{20}$$

$$R_i = \log_2\left(\frac{3P_{\mathrm{T}}^{(1)} g_i}{A^{(1)}N} + \frac{1}{N}\sum_{l=1}^{N}\frac{g_i}{g_l}\right), \quad R_i > 0 \tag{21}$$

Finally, from Equations (21) and (10), the total optimum data rate is

$$R_{\mathrm{T}}^{(1)} = \log_2\left\{\left(\frac{3P_{\mathrm{T}}^{(1)}}{A^{(1)}N} + \frac{1}{N}\sum_{l=1}^{N}\frac{1}{g_l}\right)^N \cdot \prod_{i=1}^{N} g_i\right\} \tag{22}$$

4.2. Problem 2: Minimising the total transmitting power

Let us consider a system that has to minimise the total transmitting power, under the constraints that its total data rate should not be less than a target data rate and the symbol error rate is less than a fixed error rate. Since the target is to minimise the total transmitting power, it would be necessary to reduce the data rate as much as the constraint permits. Simultaneously, the error rate should be equal to the maximum tolerable. The problem is formulated as follows:

$$\sum_{i=1}^{N} P_i \rightarrow \min \tag{23}$$

$$\sum_{i=1}^{N} R_i = R_{\mathrm{T}}^{(2)} \tag{24}$$

$$A^{(2)} = \frac{3P_i g_i}{2^{R_i} - 1} \tag{25}$$

The notations $R_{\mathrm{T}}^{(2)}$ and $A^{(2)}$ correspond to the total data rate and the fixed SER, respectively, for the second optimisation problem. First of all, the objective function Φ_2 is formulated

$$\Phi_2 = \sum_{i=1}^{N} P_i + \lambda_2 \sum_{i=1}^{N} R_i \tag{26}$$

Imposing its derivative towards P_i to be equal to zero we get Equation (27). From Equations (27) and (8), its equivalent Equation (28) is obtained

$$\frac{\partial R_i}{\partial P_i} = -\frac{1}{\lambda_2} \tag{27}$$

$$\frac{1}{\ln 2 \cdot \left(\frac{A^{(2)}}{3g_i} + P_i\right)} = -\frac{1}{\lambda_2} \tag{28}$$

Solving Equation (28) for P_i, the power distribution is

$$P_i = \frac{1}{\ln 2 \cdot \left(-\frac{1}{\lambda_2}\right)} - \frac{A^{(2)}}{3g_i} \tag{29}$$

From Equation (27) and the properties of the Leibnitz notation, we have

$$\frac{\partial P_i}{\partial R_i} = -\lambda_2 \tag{30}$$

Substituting Equation (9) into Equation (30) and solving for R_i, the bit distribution of the system that optimises the total transmission power is

$$R_i = \log_2\left(-\frac{3g_i\lambda_2}{A^{(2)} \ln 2}\right) \tag{31}$$

The Lagrange constant is calculated, substituting Equation (31) into the data rate constraint and solving the resulting equation for λ_2

DOI:10.1002/ett

$$-\lambda_2 = \frac{2^{R_T^{(2)}/N} A^{(2)} \ln 2}{3\left(\prod_{l=1}^{N} g_l\right)^{1/N}} \tag{32}$$

Substituting λ_2 into Equations (29) and (31), the power and bit distributions are attained as functions of $R_T^{(2)}$ and $A^{(2)}$.

$$R_i = \log_2\left(g_i \frac{2^{R_T^{(2)}/N}}{\left(\prod_{l=1}^{N} g_l\right)^{1/N}}\right), \quad R_i > 0 \tag{33}$$

$$P_i = \frac{A^{(2)}}{3} \cdot \frac{2^{R_T^{(2)}/N}}{\left(\prod_{l=1}^{N} g_l\right)^{1/N}} - \frac{A^{(2)}}{3g_i} \tag{34}$$

Finally, the optimal total power is from Equations (23) and (34)

$$P_T = \frac{A^{(2)} \cdot N}{3} \cdot \frac{2^{R_T^{(2)}/N}}{\left(\prod_{l=1}^{N} g_l\right)^{1/N}} - \frac{A^{(2)}}{3} \sum_{i=1}^{N} \frac{1}{g_i} \tag{35}$$

4.3. Equivalence of the solutions of the two problems

From Equations (14) and (27), it can be seen that both problems could have the same power distribution as solution if

$$\lambda_2 = \frac{1}{\lambda_1} \tag{36}$$

In fact, this is true, if the outcome (i.e. optimised quantity) of any of the two problems examined so far is imposed as constraint to the other. For instance, the optimum (minimised) overall transmission power of the second optimisation problem is imposed to be the predetermined power budget of the data rate optimisation problem. Assume that both problems have the same SER that is $A^{(1)} = A^{(2)} = A$. Therefore, we have

$$P_T^{(1)} = P_T^{(2)} \tag{37}$$

From Equations (16) and (29), we have:

$$\sum_i \left(\frac{1}{\ln 2(-\lambda_1)}\right) - \sum_i \frac{A}{3g_i} = \sum_i \left(\frac{1}{\ln 2(-1/\lambda_2)}\right) - \sum_i \frac{A}{3g_i}$$

$$\frac{N}{\ln 2 \cdot (-\lambda_1)} = \frac{N}{\ln 2 \cdot (-1/\lambda_2)}$$

and, finally, $\lambda_2 = 1/\lambda_1$ which is the sufficient condition that the two examined so far optimisation problems lead to the same power distribution. Imposing the same SER in both problems and beginning from the optimum (maximised) overall data rate of the first optimisation problem, using Equation (18), and the rate constraint of the second optimisation problem, using Equation (31) we have

$$R_T^{(1)} = R_T^{(2)} \tag{38}$$

$$\sum_i \log_2\left(-\frac{3g_i}{A^{(1)} \ln 2 \cdot \lambda_1}\right) = \sum_i \log_2\left(-\frac{3g_i\lambda_2}{A^{(2)} \ln 2}\right)$$

$$\log_2 \prod_i \left(-\frac{3g_i}{A^{(1)} \ln 2 \cdot \lambda_1}\right) = \log_2 \prod_i \left(-\frac{3g_i\lambda_2}{A^{(2)} \ln 2}\right)$$

$$\left(-\frac{3}{A^{(1)} \ln 2 \cdot \lambda_1}\right)\left(\prod_i g_i\right)^{1/N} = \left(-\frac{3 \cdot \lambda_2}{A^{(2)} \ln 2}\right)\left(\prod_i g_i\right)^{1/N}$$

and finally again $\lambda_2 = 1/\lambda_1$. That means that the two problems lead to the same bit and power distribution, when the output of one of the problems is imposed as input to the other, on condition that the SER is the same in both problems.

4.4. Problem 3: Minimising the overall symbol error rate

Suppose that a system should transmit at least $R_T^{(3)}$ bits per OFDM symbol, whereas the transmitting power should not be more than $P_T^{(3)}$. The aim is to achieve the lowest possible symbol error rate. In order to minimise the error rate, the system should be forced to work to its limits. That is, transmit as less data bits as possible using as much power as possible. Thus, the problem is formulated as follows.

$$P_{\text{error},i} = f_i(R_i, P_i) \rightarrow \min \tag{39}$$

$$\sum_{i=1}^{N} R_i = R_T^{(3)} \tag{40}$$

$$\sum_{i=1}^{N} P_i = P_T^{(3)} \tag{41}$$

Using the Lagrange method once more, function Φ is formed

DOI:10.1002/ett

$$\Phi = f_i(R_i, P_i) + \lambda_3 \sum_{i=1}^{N} R_i + \lambda_4 \sum_{i=1}^{N} P_i \tag{42}$$

The optimised system can be found solving the system of Equations (40), (41) and (43):

$$\vec{\nabla}\Phi = 0 \tag{43}$$

From Equations (43) and (42), we get the set of equations

$$\begin{aligned} \frac{\partial f_i(R_i, P_i)}{\partial R_i} + \lambda_3 = 0 \\ \frac{\partial f_i(R_i, P_i)}{\partial P_i} + \lambda_4 = 0 \end{aligned} \tag{44}$$

Imposing that $P_{\text{error},i} = P_{\text{err}}$ (i.e. constant for all subcarriers) practically means that the solution of the problem lays on the curve, defined by the surface $f_i(R_i, P_i) \ \forall R_i > 0$, $P_i > 0$ and the plane $f_i(R_i, P_i) = P_{\text{err}}$ (see Figure 2). Thus, any trivial variation of the data rate ∂R_i or the power ∂P_i per subcarrier, do not result in any variation of the error rate ∂f_i.

Therefore, the partial derivatives are equal to zero

$$\begin{aligned} \frac{\partial f_i(R_i, P_i)}{\partial R_i} = 0 \\ \frac{\partial f_i(R_i, P_i)}{\partial P_i} = 0 \end{aligned} \tag{45}$$

and, consequently, the Lagrange constants are equal to zero too.

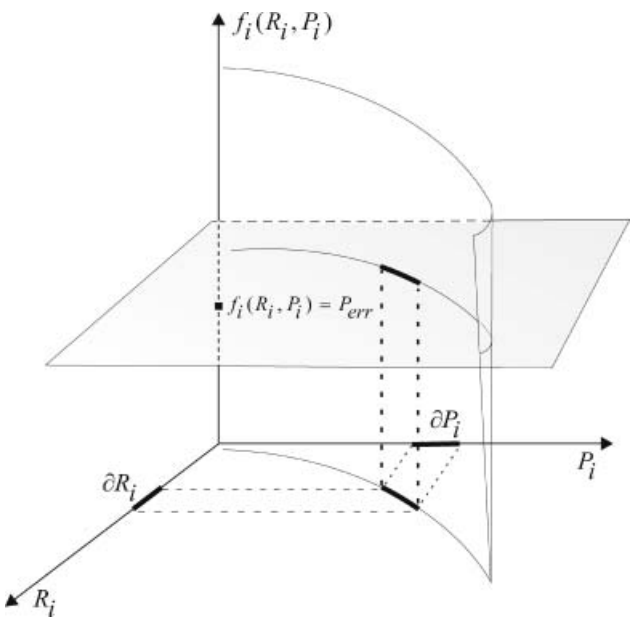

Figure 2. Schematic representation of the solution of the optimum symbol error rate system, imposing $f_i(R_i, P_i)$ to be constant for all the subcarriers.

$$\left.\begin{aligned} \lambda_3 = 0 \\ \lambda_4 = 0 \end{aligned}\right\} \tag{46}$$

Hence, the solution of the third problem is given by all sets (R_i, P_i) that satisfy the data rate constraint (40) and the power constraint (41). If the data rate constraint $R_{\text{T}}^{(3)}$ is equal to the optimum data rate $R_{\text{T}}^{(1)}$ of the first problem and the power constraint $P_{\text{T}}^{(3)}$ is equal to the respective power constraint of the first problem $P_{\text{T}}^{(1)}$, then the bit and power distributions of the first problem satisfy the constraints of the third optimisation problem and thus, those distributions are also solutions of the third problem as well. Simultaneously, if the optimum total transmission power $P_{\text{T}}^{(2)}$ of the second optimisation problem is equal to $P_{\text{T}}^{(3)}$ and the data rate constraint $R_{\text{T}}^{(3)}$ is equal to the respective data rate constraint $R_{\text{T}}^{(2)}$ of the second problem, then the solution of problem 2 is also solution of the error optimisation problem. The optimised (minimum) error rate $P_{\text{err}}^{(3)}$ is the error rate imposed as constraint into the rate or power optimisation problems ($P_{\text{err}}^{(1)}$, $P_{\text{err}}^{(2)}$, respectively). Therefore, we have shown that the pairs (20, 21) and (33, 34) are also solutions of the SER minimisation problem. The optimum SER is comprised into either $A^{(1)}$ or $A^{(2)}$. However, the error rate is the unknown and should be expressed as a function of the known $P_{\text{T}}^{(3)}$ and $R_{\text{T}}^{(3)}$. Taking Equation (34) as solution and imposing that $P_{\text{T}}^{(2)} = P_{\text{T}}^{(3)}$, $R_{\text{T}}^{(2)} = R_{\text{T}}^{(3)}$ and $A^{(2)} = A^{(3)}$, we have

$$P_{\text{T}}^{(3)} = \sum_{l=1}^{N} \left(\frac{A^{(3)} \cdot 2^{R_{\text{T}}^{(3)}/N}}{3\left(\prod_{l=1}^{N} g_l\right)^{1/N}} - \frac{A^{(3)}}{3g_l} \right) \tag{47}$$

Solving for $A^{(3)}$, the optimised quantity is obtained as a function of $P_{\text{T}}^{(3)}$ and $R_{\text{T}}^{(3)}$.

Substituting Equation (48) into Equations (33) and (34), the bit and power distribution is extracted for known total power budget and target data rate.

$$A^{(3)} = \frac{3\frac{P_{\text{T}}^{(3)}}{N} \cdot \left(\prod_{l=1}^{N} g_l\right)^{\frac{1}{N}}}{2^{\frac{R_{\text{T}}^{(3)}}{N}} - \left(\prod_{l=1}^{N} g_l\right)^{1/N} \cdot \frac{1}{N} \sum_{i=1}^{N} \frac{1}{g_i}} \tag{48}$$

$$R_i = \log_2 \left(g_i \frac{2^{R_{\text{T}}^{(3)}/N}}{\left(\prod_{l=1}^{N} g_l\right)^{1/N}} \right), \quad R_i > 0 \tag{49}$$

DOI:10.1002/ett

$$P_i = \left(\frac{2^{\frac{R_T^{(3)}}{N}}}{\left(\prod_{l=1}^{N} g_l \right)^{\frac{1}{N}}} - \frac{1}{g_i} \right) \frac{\frac{P_T^{(3)}}{N} \left(\prod_{l=1}^{N} g_l \right)^{\frac{1}{N}}}{2^{R_T^{(3)}/N} - \left(\prod_{l=1}^{N} g_l \right)^{\frac{1}{N}} \frac{1}{N} \sum_{i=1}^{N} \frac{1}{g_i}} \quad (50)$$

4.5. Remarks

At this point, we should summarise the results of the analysis so far. First of all, the rate-power function is dependent on the modulation type. Second, the rate-power function should have some certain properties. It should be one-to-one, in order to be inverted and express the power as function of the data rate. This is the case for QAM because Equation (8) is strictly increasing. The rate-power function must also be differentiable. This is also valid for Equation (8). Moreover, Equation (14) can be turned into Equation (17) if the partial derivative of the rate-power function towards P_i is not zero for any $P_i \geqslant 0$. This is also valid in QAM as the left hand side of Equation (15) is not zero for any $P_i \geqslant 0$. Finally, if the outcome of one of the three problems is imposed as input to the other, then the optimum bit and power distribution is the same.

4.6. Unified model for continuous throughput multicarrier QAM system

It is very easy to verify experimentally, the validity of our analysis and the fact that all problems lead to the same bit distribution. For this purpose, a frequency-selective channel is needed. The channel that was used as communications medium was a power line channel. In References [16] and [17], extensive measurements were performed over power lines. Two indicative transfer functions of power line channels are shown in Figure 3.

Extensive noise measurements also took place. The noise samples were stored in archives and used to calculate their variances n_i. Finally, we assumed that AWGN affects the parallel subcarriers[§] having zero mean and standard deviations $\sqrt{n_i}$. The experimental data $H_i(f_i)$ of channel 2 of Figure 3 and the noise variances n_i were used to calculate g_i using Equation (2). The tolerable error rate was fixed to 10^{-4} and the power budget was fixed to 130 μW per OFDM symbol. The OFDM symbol consists of 512 subcarriers. Iteratively, the subchannels that resulted in negative or zero bits per subcarrier, according to Equation (21) were excluded. The remainder of them was used to distribute bits. The non-integer bit distribution is shown in Figure 4.

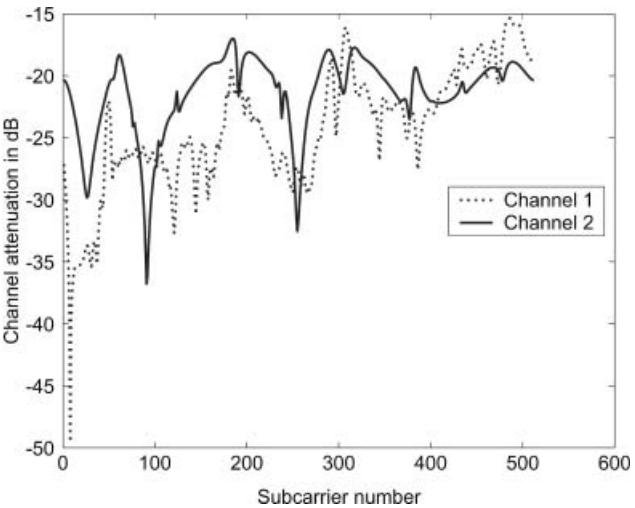

Figure 3. Typical power line transfer functions measured in the laboratory in the frequency range 500 KHz–30 MHz.

The total data rate of this simulation $R_T^{(1)} = 500$ bits per OFDM symbol was used as input into Equation (33) for the same channel 2. The resulted bit distribution is shown in Figure 5. It is identical to the bit distribution of Figure 4.

Hence, theoretically and experimentally (using simulations) it is evident that both Equations (21) and (33) lead to the same non-integer bit distribution. If we equalise the

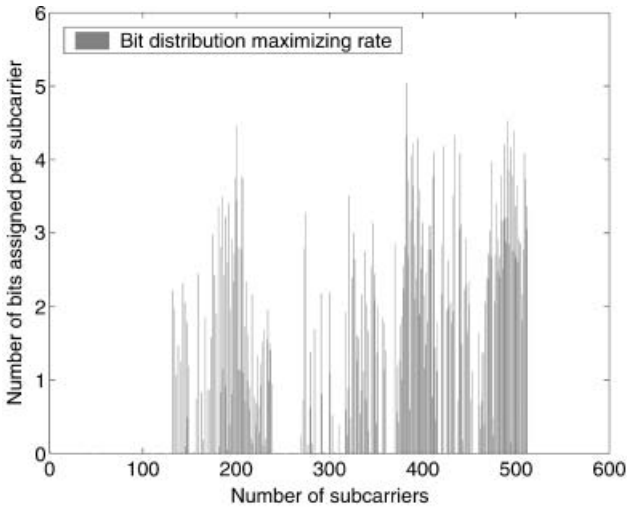

Figure 4. Non-integer bit distribution of an optimum data rate QAM–OFDM system.

[§]Adequate noise model for a power line channel has not been constructed yet. So, for simplicity reasons and without losing generality, AWGN is assumed to affect every subcarrier.

DOI:10.1002/ett

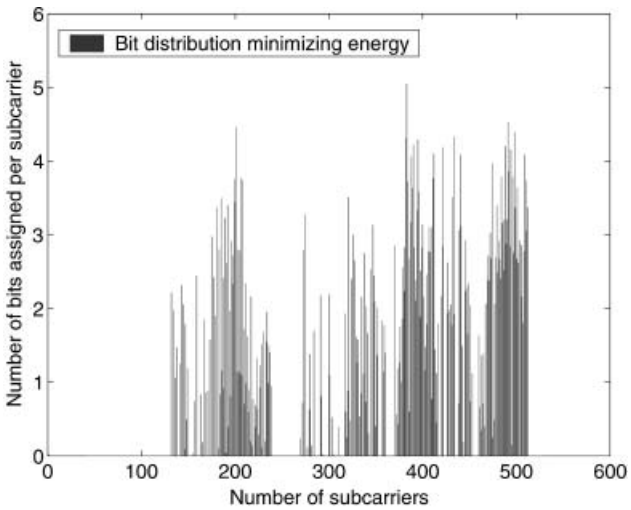

Figure 5. Non-integer bit distribution of an optimum power QAM–OFDM system.

right hand side of both of them, a useful model that describes the overall OFDM system is attained. The constant SER of all the subcarriers is a function of the total data rate and the total transmitting power. Equation (51) provides the continuous throughput QAM–OFDM model.

$$P_{\text{err}} = 4Q\left(\sqrt{A}\right), \text{ where } A = \frac{3P_{\text{av}}\text{GM}_{g_i}}{2^{R_{\text{av}}} - \text{GM}_{g_i}\text{MI}_{g_i}} \qquad (51)$$

GM_{g_i} is the geometric mean of the subchannel to noise ratios g_i, MI_{g_i} is the mean value of the inverse subchannel to noise ratios g_i^{-1} and P_{av} and R_{av} are the average power and bit rate that is transmitted per subcarrier, of the N subcarriers that remained turned on.

Obviously, the A parameter of Equation (51) is the same with Equation (48), which gives the solution of the third optimisation problem. Thus, Equation (51) unifies the solutions of all problems into one simple equation. If the subchannels that are turned on are determined, then channel's statistics such as the geometric mean of the subchannel to noise ratios, and the mean value of the inverse of the subchannel to noise ratios are enough to allow evaluating the system's performance.

4.7. Comments on the continuous throughput QAM–OFDM model

Some important comments on the continuous throughput QAM–OFDM model are:

(1) Equation (51) seems to be analogous to Equation (7) for single-carrier QAM.
(2) Equation (51) describes the performance of the N parallel QAM subcarriers loaded, using either Equations (21) or (33) and the global parameters. The whole frequency bandwidth is manipulated using some statistical characteristics of it, like the geometric mean of the subchannel to noise ratios g_i and the mean value of the noise to subchannel ratios $1/g_i$. These statistics, in fact, summarise the influence of the frequency band over the multicarrier system.
(3) Equation (51) is expected to be rather pessimistic, compared to the performance of a real QAM–OFDM loaded system, due to the fact that the corresponding for one subcarrier model (7) is an upper bound for the error rate.

The graphical representation of Equation (51) for data rates fluctuating from 1000 up to 3000 bits per OFDM symbol and power budget 1 mW is shown in Figure 6. The transmission medium was channel 2 of Figure 3.

4.8. Unified model versus integer throughput multicarrier QAM system

The real bit distribution is practically unacceptable. It has to be rounded to integers. The model that describes the resulted integer throughput system is of greater importance as it has practical applicability. Except of the category of the algorithms that lead to integer bit distributions (like the algorithms proposed in References [9, 10]), all the other

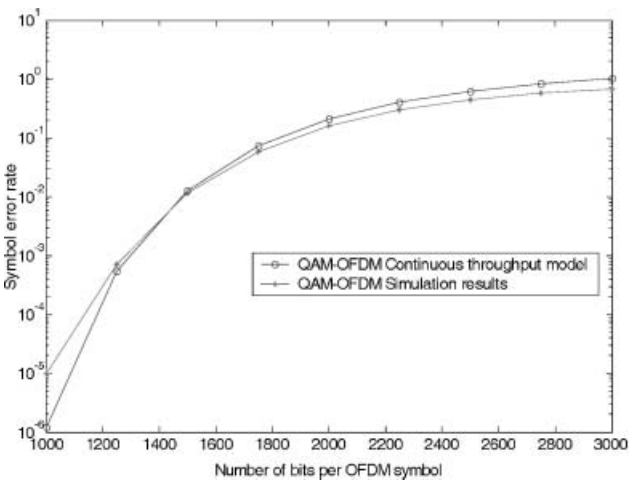

Figure 6. Optimum symbol error rate of an adaptive QAM–OFDM system, using simulations and the continuous throughput model.

DOI:10.1002/ett

algorithms [4, 6, 7, 13] approach the final integer bit distribution, rounding a non-integer bit distribution. In Figure 6, we present the results of the simulated QAM–OFDM system that minimises the error rate, using Equations (49) and (50) for several data rates and constant power budget equal to $P_T = 1\,\text{mW}$.

The channel that is used is channel 2 of Figure 3. The non-integer bit distribution was rounded using the rounding procedure proposed in Reference [8]. For every simulation run, the symbol error rate was counted. As expected, Equation (51) provides an upper bound of the performance of the actual system, by virtue for most data loads. Moreover, the simulated system is diverted from the optimum solution as the rounding procedure distracts it from optimality. However, the difference between the simulation curve (integer throughput system) and the modelled curve (51) is not important for most of the data loads. Figure 6 shows that the continuous throughput model tracks the real system closely.

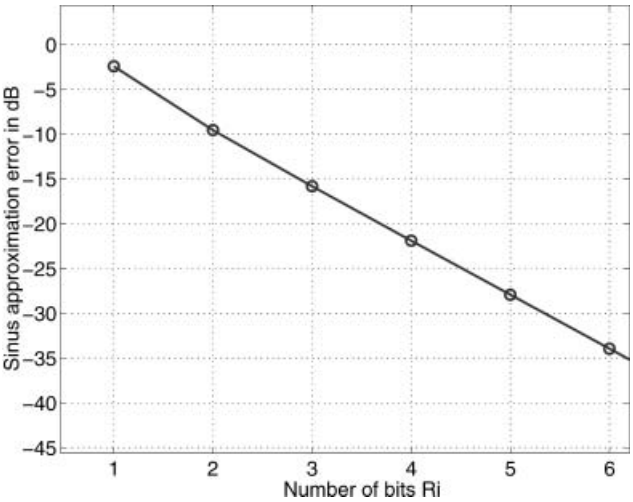

Figure 7. The approximation error in dB, introduced by substituting the sinus function with its argument, versus the number of bits.

5. PSK APPLICATION

In this part of the paper, the same methodology is used to solve again the optimisation problems and prove that all of them, under certain pre-requirements, lead to the same bit distributions. The function that implicates bit rate, power and symbol error rate per subcarrier [2] is

$$P_{\text{error},i} = 2Q\left(\sin\left(\frac{\pi}{2^{R_i}}\right)\sqrt{2P_i g_i}\right) \tag{52}$$

For simplicity reasons and in order to transform Equation (52) into a more convenient form, the sinus function is substituted by its argument.

$$P_{\text{error},i} = 2Q\left(\frac{\pi}{2^{R_i}}\sqrt{2P_i g_i}\right) \tag{53}$$

It is well known that $\sin x \approx x$ when $x \ll 1$. In PSK, this is the case for $R_i \geqslant 2$. Indeed, Figure 7 plots the approximation error $(\frac{\pi}{2^{R_i}} - \sin\frac{\pi}{2^{R_i}})/\sin\frac{\pi}{2^{R_i}}$ expressed in dB for $R_i \in [1, \ldots, 6]$. For $R_i \geqslant 2$, the approximation error is less than $-10\,\text{dB}$, whereas for $R_i = 1$ the error is $-2.4\,\text{dB}$. Because of the fact that $\pi/2^{R_i} > \sin(\pi/2^{R_i})$ for $R_i \geqslant 0$, Equation (53) leads to a system with optimistic performance. The theoretical results, that is SER, are expected to be better compared to the actual system performance.

In order to manipulate Equation (53) easier, its argument that implicates the SER, the transmission power and the number of bits per subcarrier is isolated into Equation (54).

$$A = \frac{\pi}{2^{R_i}}\sqrt{2P_i g_i} \tag{54}$$

The system that is examined has equal SER among its subcarriers $P_{\text{error},i} = P_{\text{err}}$ and thus $A = Q^{-1}(P_{\text{err}}/2)$.

Equation (54), solved for R_i, gives the rate-power function for PSK modulation

$$R_i = \log_2\left(\frac{\pi}{A}\sqrt{2P_i g_i}\right) \tag{55}$$

Equation (55) is strictly increasing and thus, it is invertible. The inverse function is

$$P_i = \frac{A^2}{\pi^2}\frac{2^{2R_i}}{2g_i} \tag{56}$$

Equations (55) and (56) are differentiable once. Differentiating them once, Equations (57) and (58) are obtained, respectively

$$\frac{\partial R_i}{\partial P_i} = \frac{1}{2\ln 2 \cdot P_i} \tag{57}$$

$$\frac{\partial P_i}{\partial R_i} = \frac{A^2}{\pi^2 g_i}2^{2R_i}\ln 2 \tag{58}$$

5.1. PSK maximising rate

The optimisation problem is the same as Section 4.1 states. We follow the same methodology using the

DOI:10.1002/ett

objective function Φ_1. Substituting Equation (57) into (14), we get

$$-\lambda_1 = \frac{1}{2\ln 2 \cdot P_i} \tag{59}$$

The Lagrange multiplier is calculated solving Equation (59) for P_i and using it in the power constraint (11)

$$-\lambda_1 = \frac{N}{2\ln 2 \cdot P_{\mathrm{T}}^{(1)}} \tag{60}$$

The power distribution is obtained from Equations (60) and (59)

$$P_i = \frac{P_{\mathrm{T}}^{(1)}}{N} \tag{61}$$

Finally, using Equations (61) and (55), the bit distribution is

$$R_i = \log_2\left(\frac{\pi}{A^{(1)}}\sqrt{2\frac{P_{\mathrm{T}}^{(1)}}{N}g_i}\right), \quad R_i > 0 \tag{62}$$

5.2. PSK minimising power

The optimisation problem is the same as Section 4.2 states. We follow the same methodology using the objective function Φ_2. Substituting Equation (58) into Equation (30), we obtain Equation (63)

$$-\lambda_2 = \frac{(A^{(2)})^2}{\pi^2 g_i} 2^{2R_i} \ln 2 \tag{63}$$

The Lagrange multiplier λ_2 is calculated solving Equation (63) for R_i and using it in the rate constraint (24).

Afterward, the bit distribution is acquired using Equations (63) and (64)

$$-\lambda_2 = \frac{2^{2R_{\mathrm{T}}^{(2)}/N}(A^{(2)})^2 \ln 2}{\pi^2\left(\prod_{l=1}^{N} g_l\right)^{1/N}} \tag{64}$$

$$R_i = \frac{1}{2}\log_2\left(g_i \frac{2^{\frac{2R_{\mathrm{T}}^{(2)}}{N}}}{\left(\prod_{l=1}^{N} g_l\right)^{1/N}}\right), \quad R_i > 0 \tag{65}$$

Finally, according to Equation (56), using Equation (65), the power distribution is obtained

$$P_i = \frac{(A^{(2)})^2}{\pi^2}\frac{2^{2R_{\mathrm{T}}^{(2)}/N}}{2\left(\prod_{l=1}^{N} g_l\right)^{1/N}} \tag{66}$$

Note that from Equation (66), we have a constant power distribution to the subcarriers of a PSK adaptive OFDM system, just like Equation (61) shows. Thus, for common SER $A^{(1)} = A^{(2)} = A$, if the optimised quantity of the power minimisation problem is imposed to the rate maximisation problem, we have:

$$P_{\mathrm{T}}^{(1)} = P_{\mathrm{T}}^{(2)}$$

$$P_{\mathrm{T}}^{(1)} = \frac{N \cdot A^2}{\pi^2}\frac{2^{2R_{\mathrm{T}}^{(2)}/N}}{2\left(\prod_{l=1}^{N} g_l\right)^{1/N}} \tag{67}$$

and substituting it in Equation (62), we have for the bit distribution of the rate optimisation problem

$$R_i = \frac{1}{2}\log_2\left(g_i \frac{2^{\frac{2R_{\mathrm{T}}^{(2)}}{N}}}{\left(\prod_{l=1}^{N} g_l\right)^{1/N}}\right) \tag{68}$$

which means that the bit distributions of the two problems are identical.

5.3. PSK minimising symbol error rate

According to the analysis in Section 4.4, either Equations (61, 62) or Equations (65, 66) can be used as solutions of the third optimisation problem. The optimum error rate is entailed into either $A^{(1)}$ or $A^{(2)}$. Nevertheless, the error rate is the unknown and should be expressed as a function of the known $P_{\mathrm{T}}^{(3)}$ and $R_{\mathrm{T}}^{(3)}$. From Equations (65) and (61), the bit and power distribution is

$$R_i = \frac{1}{2}\log_2\left(g_i \frac{2^{2R_{\mathrm{T}}^{(3)}/N}}{\left(\prod_{l=1}^{N} g_l\right)^{1/N}}\right), \quad R_i > 0 \tag{69}$$

$$P_i = \frac{P_{\mathrm{T}}^{(3)}}{N} \tag{70}$$

The unknown $A^{(3)}$ is given as function of $P_{\mathrm{T}}^{(3)}$ and $R_{\mathrm{T}}^{(3)}$ by Equation (71). The latter equation originates from

DOI:10.1002/ett

Equation (66), summing both sides over all N subcarriers and replacing $A^{(2)} = A^{(3)}$ and $R_{\mathrm{T}}^{(2)} = R_{\mathrm{T}}^{(3)}$.

$$A^{(3)} = \frac{\pi}{2^{R_{\mathrm{T}}^{(3)}/N}} \sqrt{2\frac{P_{\mathrm{T}}^{(3)}}{N}\left(\prod_{l=1}^{N} g_l\right)^{1/N}} \tag{71}$$

5.4. Unified model for continuous throughput multicarrier PSK system

The validity of the prior theoretic analysis is tested experimentally. The channel that was used was again channel 2 of Figure 3. The tolerable symbol error rate was fixed to 10^{-4} and the power budget was fixed to 117 μW per OFDM symbol. Iteratively, the subchannels that resulted in negative or zero bits per subcarrier, according to Equation (62) were closed. The remained turned on were loaded with bits. The $R_{\mathrm{T}}^{(1)}$ output of this system, equal to 500 bits, is used as input in Equation (65) and after closing the 'bad' subcarriers, we distribute bits over the rest of them. Figures 8 and 9 present the continuous bit distributions resulted from Equations (62) and (65). They are identical.

Therefore, the theoretic analysis has been verified via simulations. Equalising the right hand side of both Equations (62) and (65), a useful model that describes the overall PSK–OFDM system is obtained. Equation (72) is the continuous throughput PSK–OFDM model. The constant error rate of all subcarriers is a function of the total data rate and the total transmitting power.

$$A = \frac{\pi}{2^{R_{\mathrm{av}}}} \sqrt{2P_{\mathrm{av}}\mathrm{GM}_{g_i}} \rightarrow P_{\mathrm{err}} = 2Q(A) \tag{72}$$

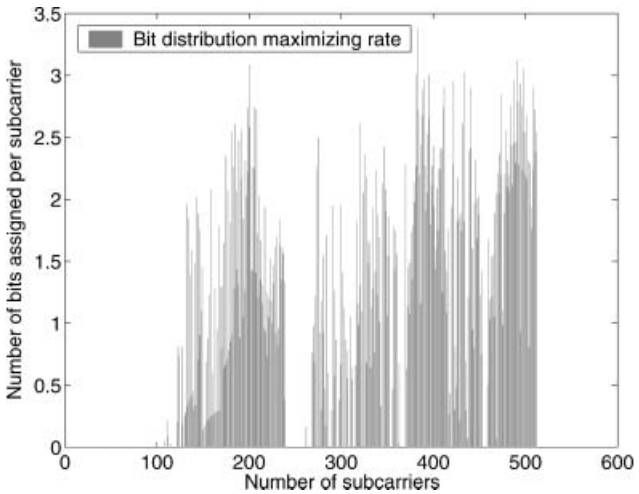

Figure 8. Non-integer bit distribution of an optimum data rate PSK–OFDM system.

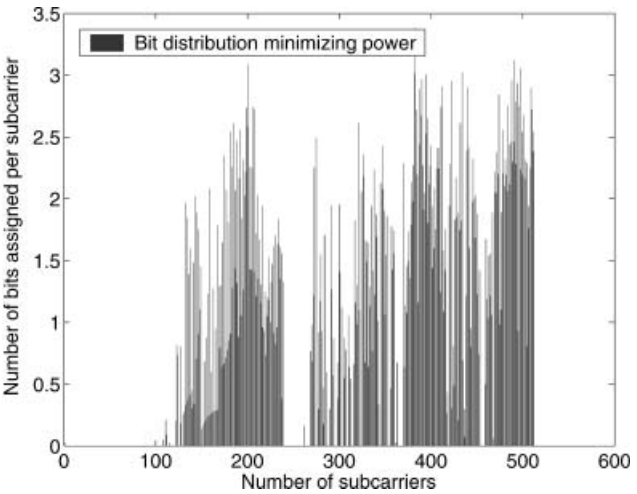

Figure 9. Non-integer bit distribution of an optimum power PSK–OFDM system.

P_{av} and R_{av} are the average power and bit rate that are distributed over the N remained turned on subcarriers. GM_{g_i} is the geometric mean of the subcarrier to noise ratios g_i of those 'good' subcarriers. Please notice that the general model (72) is completely analogous to Equation (54), used for one subcarrier modulated with PSK. However, as mentioned earlier, the theoretical model that Equation (72) introduces is rather optimistic describing the system's performance. Moreover, Equation (72) is the same as Equation (71), which gives the solution of the third optimisation problem. Thus, Equation (72) unifies the solutions of all problems into one simple equation. Its graphical representation for several data rates, fluctuating between 1000 and 3000 bits per OFDM symbol and constant power budget fixed at $P_{\mathrm{T}} = 1$ mW is shown in Figure 10. The channel that is used is channel 2 of Figure 3.

5.5. Unified model versus integer throughput multicarrier PSK system

In this subsection, a PSK system loaded using Equations (69) and (70) is simulated. The channel that is used is again channel 2. The continuous bit distribution is rounded using the procedure described in Reference [8]. Then, for every simulation run, the actual symbol error rate is counted for several data rates fluctuating between 1000 and 3000 bits per OFDM symbol and constant power budget equal to $P_{\mathrm{T}} =$ 1 mW. The simulation results are plotted in Figure 10.

DOI:10.1002/ett

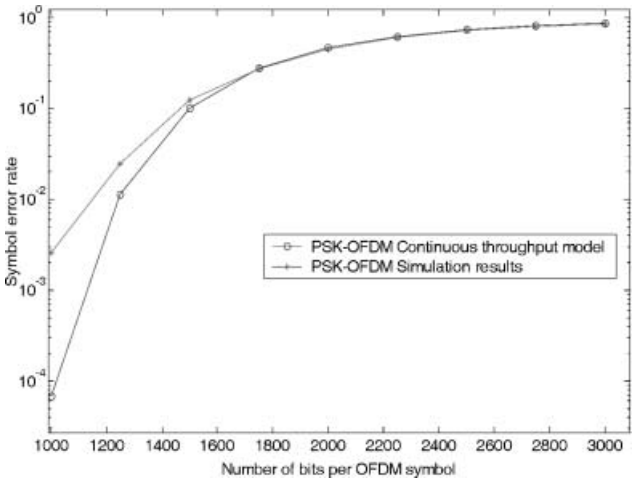

Figure 10. Optimum symbol error rate of an adaptive PSK–OFDM system, using simulations and the continuous throughput model.

Please notice that the theoretic continuous throughput model, that is Equation (72) tracks the simulated system closely. Second, the model is optimistic compared to the actual system as expected. It is diverted in the lower part of the plot where few data bits are loaded. This is attributed to the fact that the approximation error in Equation (53) is important for $R_i < 2$. For instance, 1000 bits per OFDM symbol when 512 subcarriers are used means that $R_{\text{av}} < 2$ and the approximation error, according to Figure 7, is great. This error diverts the theoretical model from the actual system. Moreover, it is expected that the integer-rounding procedure also diverts slightly the system from the optimum continuous solution.

6. CONCLUSIONS

In this paper, the performance of the optimum adaptive OFDM systems are unified into simple models. Those models are dependent on the modulation type that is used. We have examined the QAM and the PSK cases, as they are of major practical interest. The unified models that were constructed for every modulation type are the so-called continuous throughput models because the subcarriers are allowed to be loaded with non-integer number of bits. The continuous throughput models are very useful because of their simplicity. They can be used to handle a multicarrier system, in a way similar to single-carrier systems. Whole frequency bands are characterised by average statistics like the geometric mean of the subchannel to noise ratios and the mean value of the noise to subchannel ratios. Moreover, the integer throughput multicarrier systems are found to be rather close to the continuous throughput systems. This is very important because the continuous throughput system, although unacceptable in most applications, it can be used to predict the performance of an integer throughput system.

The difference between the models and the actual systems becomes trivial with the data load increase. That means that when the system is pushed to work to its limits (severe circumstances), the models offer a good approximation tool, in order to design a multicarrier system without needing to run the bit-loading algorithms to their extend. The quantification of the difference of the performance of the continuous throughput and the integer throughput system is an issue for further work.

REFERENCES

1. Bingham JAC. Multicarrier modulation for data transmission: An idea whose time has come. *IEEE Communications Magazine* 1990; **28**(5):5–14 (DOI 10.1109/35.54342).
2. Proakis JG. *Digital Communications.* McGraw Hill: New York, 1995, 278–282.
3. Piazzo L. Optimum adaptive OFDM systems. *European Transactions on Telecommunications* 2003; **14**(3):205–212 (DOI: 10.1002/ett.919).
4. Chow PS, Cioffi JM, Bingham JAC. A practical discrete multitone tranceiver loading algorithm for data transmission over spectrally shaped channels. *IEEE Transactions on Communications* 1995; **43**(2–4):773–775 (DOI 10.1109/26.380108).
5. Baccarelli E, Fasano A, Biagi M. Novel efficient bit-loading algorithms for peak-energy-limited ADSL-type multicarrier systems. *IEEE Transactions on Signal Process* 2002; **50**(5):1237–1247 (DOI 10.1109/78.995090).
6. Fischer RFH, Huber JB. A new loading algorithm for discrete multitone transmission. In *Proceedings of IEEE Globecom* 1996; **1**:724–728 (DOI 10.1109/GLOCOM.1996.594456).
7. Leke A, Cioffi J. A maximum rate loading algorithm for discrete multitone modulation systems. In *Proceedings of IEEE Globecom. 1997*, 1514–1518 (DOI 10.1109/GLOCOM.1997.644387).
8. Assimakopoulos C, Pavlidou FN. Integrated rounding method for real number bit distribution over DMT systems. *IEE Electronics Letters* 2004; **40**(19):1235–1236 (DOI 10.1049/el:20045830).
9. Hughes-Hartogs D. Ensemble Modem Structure for Imperfect Transmission Media. U.S. Pats. Nos. 4,679,227 (July 1987), 4,731,816 (March 1988), and 4,833,796 (May 1989).
10. Baccarelli E, Biagi M. Optimal integer bit-loading for multicarrier ADSL systems subject to spectral-compatibility limits. *Signal Processing (EURASIP)* 2004; **84**(4):729–741.
11. Piazzo L. Fast algorithm for power and bit allocation in OFDM systems. *Electronics Letters* 1999; **35**(25):2173–2174 (DOI 10.1049/el:19991516).
12. Sonalkar RV, Shively RR. An efficient bit-loading algorithm for DMT applications. *IEEE Communications Letters* 2000; **4**(3):80–82 (DOI 10.1109/4234.831031).
13. Czylwik A. Adaptive OFDM for wideband radio channels. In *Proceedings of IEEE Globecom*, 1996; **1**:713–718 (DOI 10.1109/GLOCOM.1996.594454).

14. Krongold BS, Ramchandran K, Jones DL. Computationally efficient optimal power allocation algorithms for multicarrier communication systems. *IEEE Transactions on Communications* 2000; **48**(1):23–27 (DOI 10.1109/26.818869).
15. Kalet I. The multitone channel. *IEEE Transactions on Communications* 1989; **37**(2):119–124 (DOI 10.1109/26.20079)
16. Assimakopoulos C, Pavlidou FN. Measurements and Modeling of In-House Power Lines Installation for Broadband Communications. In *Proceedings of the 5th ISPLC*, 2001, 73–78.
17. Assimakopoulos C, Katsis PL, Pavlidou FN, Obradovic D, Obradovic M. xDSL Techniques for Power Line Communications. In *Proceedings of the 7th ISPLC*, 2003, 21–25.

AUTHORS' BIOGRAPHIES

Costas Assimakopoulos has received his diploma in Electrical and Computer Engineering from the Aristotle University of Thessaloniki, Greece in 2000. He is currently a Ph.D. candidate in the same department. His research interest involves multicarrier transmission techniques and coding. He has also studied Power Lines used as communications media. He was also scientific secretary of the 6th International Symposium on Power Line Communications and its Applications (ISPLC 2002) that was held in Athens. He is a member of the IEEE and the Technical Chamber of Greece.

Fotini-Niovi Pavlidou received her Ph.D. in Electrical Engineering from the Aristotle University of Thessaloniki, Greece, in 1988 and the Diploma in Mechanical-Electrical Engineering in 1979 from the same institution. She is currently a full Professor at the Department of Electrical and Computer Engineering at the Aristotle University. Her research interests are in the field of mobile and personal communications, satellite communications, multiple-access systems, routing and traffic flow in networks and QoS studies for multimedia applications over the Internet. She is involved in many national and international projects in these areas (Tempus, COST, Telematics, IST). She has served as member of the TPC in many IEEE/IEE conferences. She is a permanent reviewer for many international journals. She has published about 80 papers in refereed journals and conferences. She is a senior member of IEEE, currently chairing the joint IEEE VT&AES Chapter in Greece.